FOI-R--1398--SE
April 2005
ISSN 1650-1942

FOI
SWEDISH DEFENCE
RESEARCH AGENCY

Base Data Report

Visualization of the elastic blade motion of an operating wind turbine

Göran Ronsten

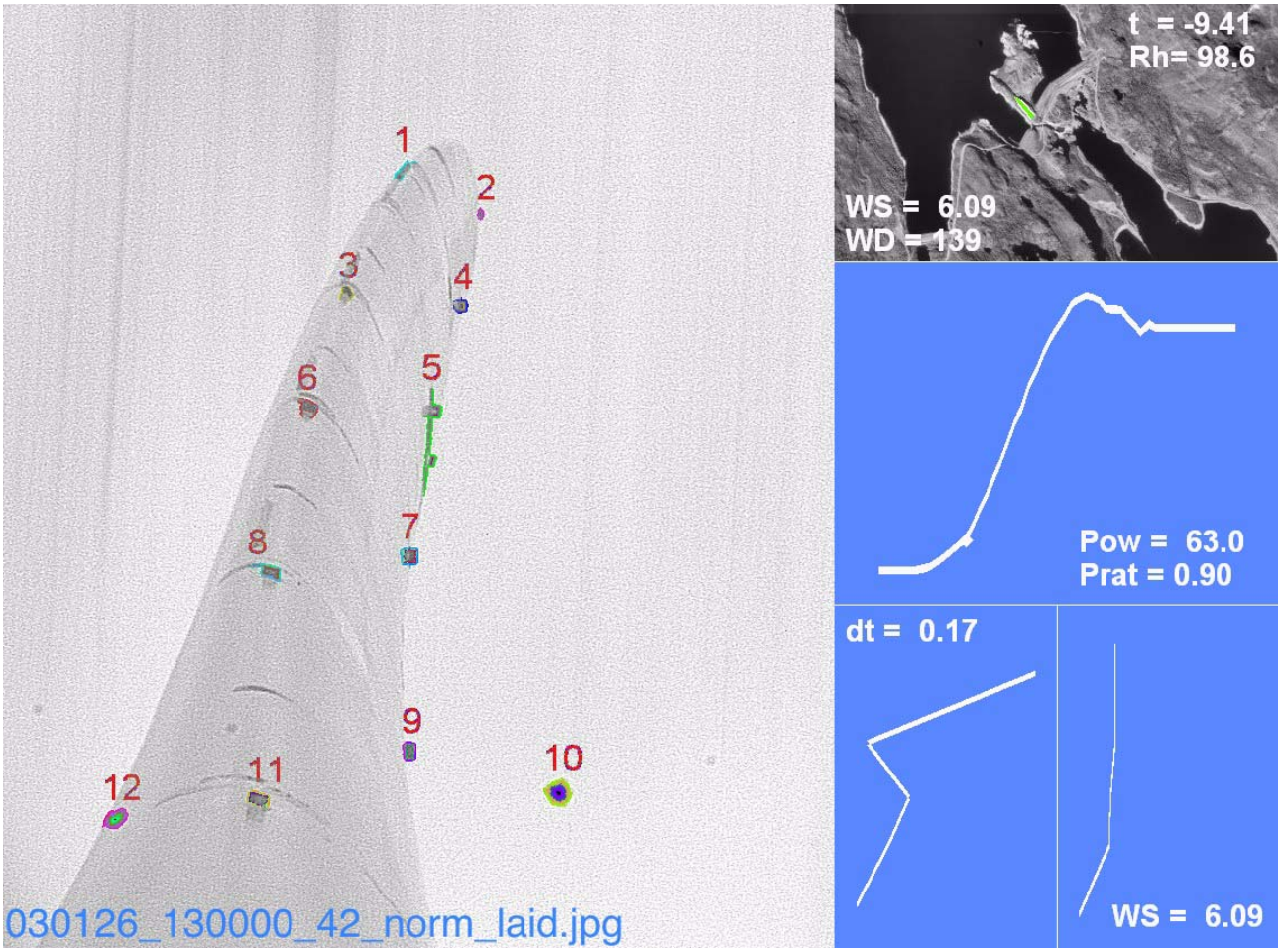

Visualization of the elastic blade motion of an operating wind turbine

Göran Ronsten

Issuing organization
FOI – Swedish Defence Research Agency
Division of Aeronautics, FFA
SE - 172 90 Stockholm

Report number, ISRN
FOI-R--1398--SE

Report type
Base data report

Research area code
Civil applications

Month year
April 2005

Project no.
E870363

Customers code
Civil applications

Sub area code
Contracted Research

Author/s (editor/s)
Göran Ronsten

Project manager
Göran Ronsten

Approved by
Björn Montgomerie

Scientifically and technically responsible
Göran Ronsten

Report title (In translation)

Visualization of the elastic blade motion of an operating wind turbine

Abstract (not more than 200 words)

Blade elastic displacement were successfully tracked by means of digital photographic recording using both Light Emitting Diods; LEDs, and reflexes mounted on a wind turbine blade. A procedure for image analysis was developed. The output from the image analysis was co-ordinates of the objects under investigation. Although the method developed is useful in producing results it still remains to verify the integrity of the results versus, for example, load measurements. The image analysis carried out and presented in this report shows that verification of simulation of blade movements is attainable. However, exact outdoor inflow conditions are extremely difficult to measure and it is therefore not possible to emulate every situation in detail. An increased knowledge of actual blade translation and rotation will nevertheless enable improvement of structural dynamics simulation codes. This is an insight which will grow with the size of future turbines.

Keywords

wind energy, blade motion, image analysis

Further bibliographic information

Language English

ISSN 1650-1942

Pages 42 p.

Distribution: STEM (3) + FOI distribution list

Price acc. to pricelist

Security classification: Open

Utgivare Totalförsvarets Forskningsinstitut - FOI Avdelningen för Systemteknik 172 90 Stockholm	**Rapportnummer, ISRN** FOI-R--1398--SE	**Klassificering** Underlagsrapport
	Forskningsområde 9 Övriga civila tillämpningar	
	Månad, år April 2005	**Projektnummer** E870363
	Verksamhetsgren 91 Övriga civila tillämpningar	
	Delområde 5 Uppdragsfinansierad verksamhet	
Författare/redaktör Göran Ronsten	**Projektledare** Göran Ronsten	
	Godkänd av Björn Montgomerie	
	Tekniskt och/eller vetenskapligt ansvarig Göran Ronsten	

Rapportens titel

Visualization of the elastic blade motion of an operating wind turbine

Sammanfattning (högst 200 ord)

Ett vindturbinblads rörelser har framgångsrikt analyserats med hjälp av digital kamerateknik kombinerad med på bladet monterade fixpunkter. För att nå ända fram har en metod, baserad på kommersiellt tillgänglig bildanalysprogramvara, för att analysera bilderna utvecklats Projektresultatet utgörs av koordinater för bladets fixpunkter. Däremot ingick det inte i detta projekt att verifiera bladrörelser mot uppmätta lastsignaler även om sådana simultana lastmätningar har genomförts. En fullständigt korrekt simulering av en vindturbins bladrörelser kräver idag alltför detaljerad kunskap om såväl vindfält som aggregategenskaper. Resultaten från simuleringar och mätningar måste därför idag bearbetas bearbetas statistiskt. Behovet av ökad kunskap om bladets verkliga rörelser kommer att växa allteftersom aggregaten växer i storlek.

Nyckelord

Vindkraft, bladrörelse, bildanalys

Övriga bibliografiska uppgifter	**Språk** Engelska
ISSN 1650-1942	**Antal sidor:** 42
Distribution: STEM (3) + enligt missiv	**Pris:** Enligt prislista **Sekretess:** Öppen

Abstract

Simulation of blade movements is nowadays a standard procedure used to design new wind turbine rotors as well as for verifying design load cases. The author's ambition was to investigate the possibility to verify blade displacements and twist by means of digital photographic recording. The equipment chosen was state-of-the-art at the time when the project was started in 2001. Similar measurements were initiated in two EU-projects, [4] and [5]. Real-time evaluation of the tower movements have been presented in [3]. However, no official results concerning image analysis of blade motion have been presented by these projects.

Recent technical development in digital camera and computer technology has made the hardware solution chosen somewhat old fashioned. High resolution cameras now connect via "simple" serial data buses like IEEE1394 and USB 2.0. Edge detection software, a crucial part in digital image analysis, is still part of expensive software packages. This last digital fortress is about to change with modern operating systems like MacOSX 10.4 where such features are an integrated part of the operating system. Any future application of methods based on digital imagery has been greatly facilitated from the recent rapid development of these techniques.

Icing was investigated by analysis of measured data. Simultaneous load measurements and images were acquired. These data remain to be evaluated jointly. The load measurements have been analyzed in [1]. This report describes the steps taken to obtain the measurements of elastic blade displacement.

FOI
TOTALFÖRSVARETS
FORSKNINGSINSTITUT

Address:
FOI
172 90 Stockholm
SWEDEN

Phone: +46-855503000

Acknowledgements

This work has been co-financed by STEM, The Swedish Energy Agency under contract P13650-1 and The Swedish Defence Research Agency (FOI). The author is grateful for the support given by the financing bodies.

Table of contents

1 Conclusions

Blade elastic displacement were successfully tracked by means of digital photographic recording using both Light Emitting Diods; LEDs, and reflexes mounted on a wind turbine blade, **Figure 41and Figure 42**. A procedure for image analysis was developed using LabView, a software from National Instruments. The output from the image analysis was co-ordinates of the objects under investigation. Although the method developed is useful in producing results it still remains to verify the integrity of the results versus, for example, load measurements.

The equipment chosen was state-of-the-art at the time when the project was started in 2001. Similar measurements were initiated in two EU-projects, [4] and [5]. Real-time evaluation of the tower movements have been presented in [3]. However, no official results from these projects have been presented concerning image analysis of blade motion. The future development of verification methods based on visual inspection will greatly benefit by the recent fast paced development in hardware and software.

The image analysis carried out and presented in this report shows that verification of simulation of blade movements is attainable. However, exact outdoor inflow conditions are extremely difficult to measure and it is therefore not possible to emulate every situation in detail. The technique of comparison between simulation and measurement must therefore be based on statistical methods.

An increased knowledge of actual blade translation and rotation will nevertheless enable improvement of structural dynamics simulation codes. This is an insight which probably will grow with the size of future turbines.

Icing was investigated by analysis of measured data. Simultaneous load measurements and images were acquired. However, these data remain to be evaluated jointly. Measured load data are evaluated in [1]. An increased amplitude at two per revolution (2P) in the rotating system was found in assumed icing conditions. 2P in a rotating system implies an increase in 1P amplitude in a (more or less) fixed co-ordinate system such as in the nacelle or tower.

2 Description of the measurement system

The measurement system consists of one ordinary office computer for data storage, one purpose built smaller computer and a camera mounted behind a rotating glass window for continuos centrifugal cleaning. Power to the hub mounted computer is supplied via slip rings whereas data communication is transferred via a wireless network to the nacelle and further on via cable to the storage computer, Figure 1.

2.1 Equipment in hub and nacelle

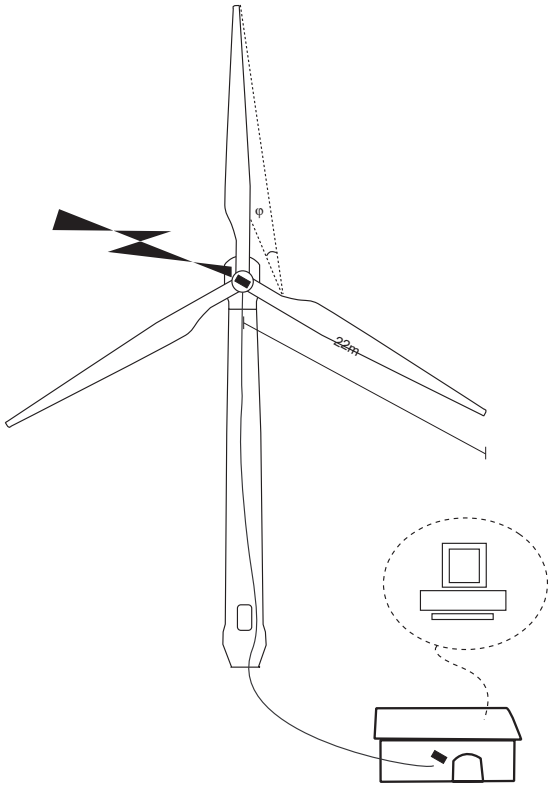

Figure 1. Measurement system set-up. Data communication is transferred via a wireless network to the nacelle and further on via cable to the storage computer.

Components of the measurement system are presented on the following pages.

Figure 2. Mounting frame, hub computer.

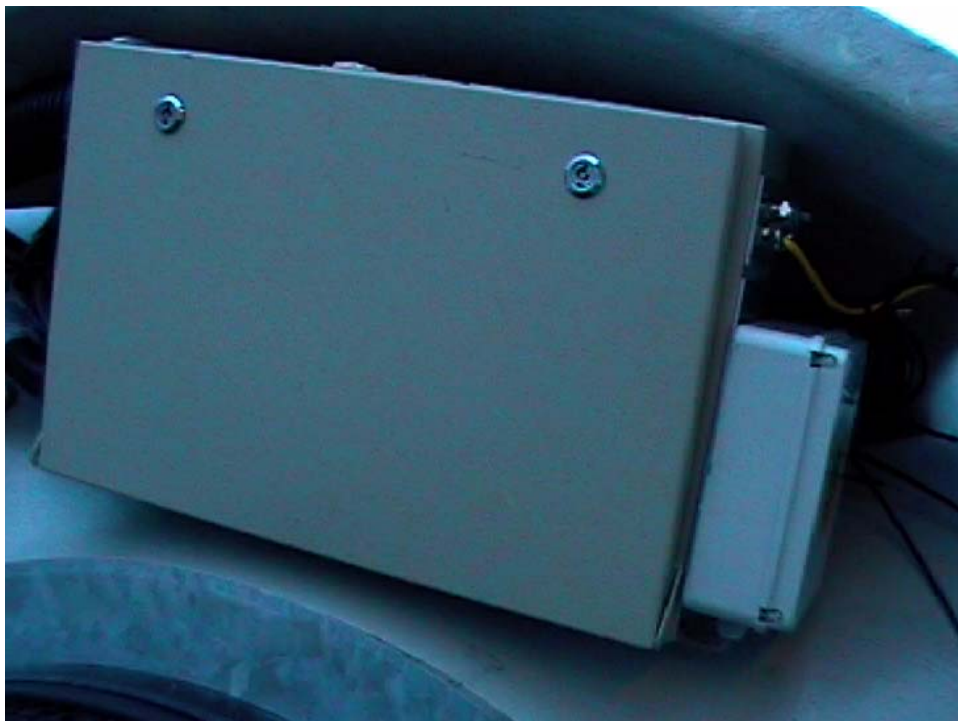

Figure 3. Hub computer. The box on the right contains electronics to control the camera lens.

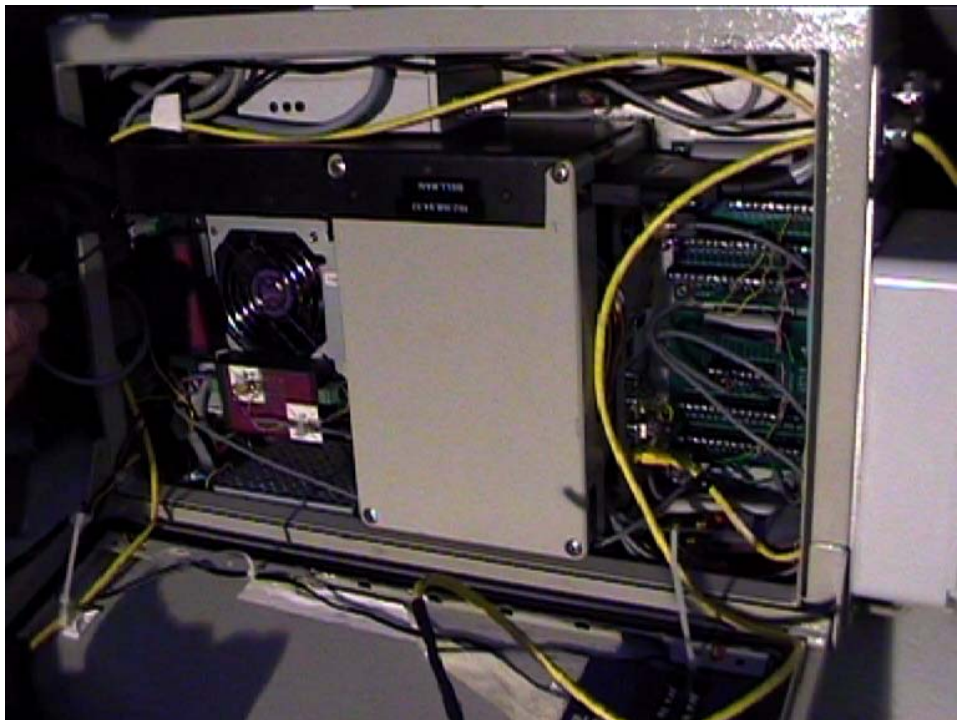

Figure 4. Hub mounted box containing power supply (left), a 500 MHz PII computer (middle), measurement signal connector (right) and camera interface (on top).

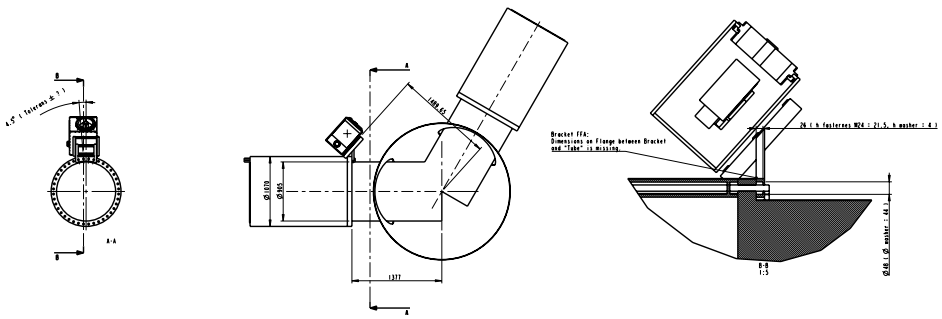

Figure 5. Drawing of camera mounting on flange of blade.

Figure 6. Attachment of camera house.

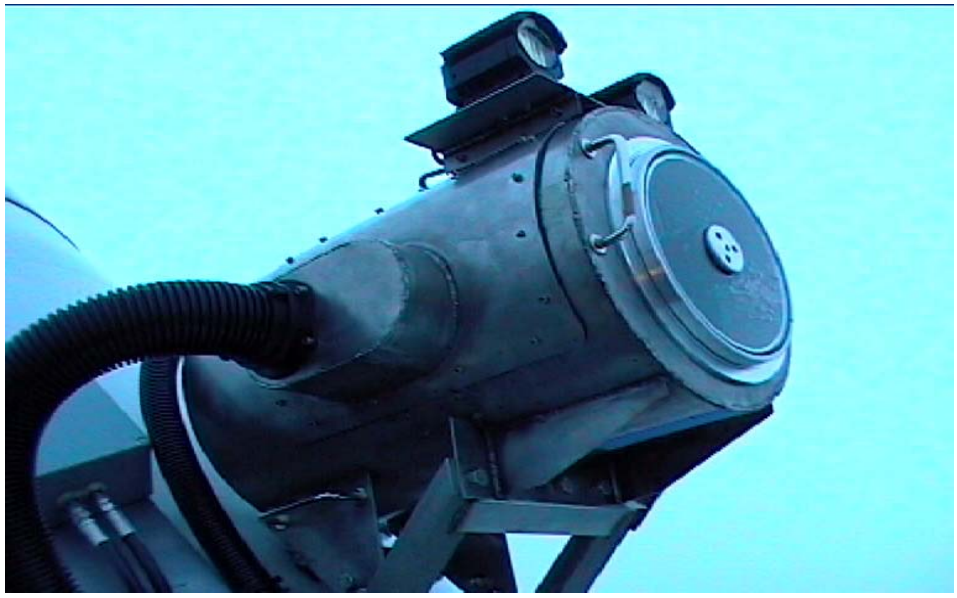

Figure 7. The camera house is equipped with a rotating clear view screen and a 400 W heating element.

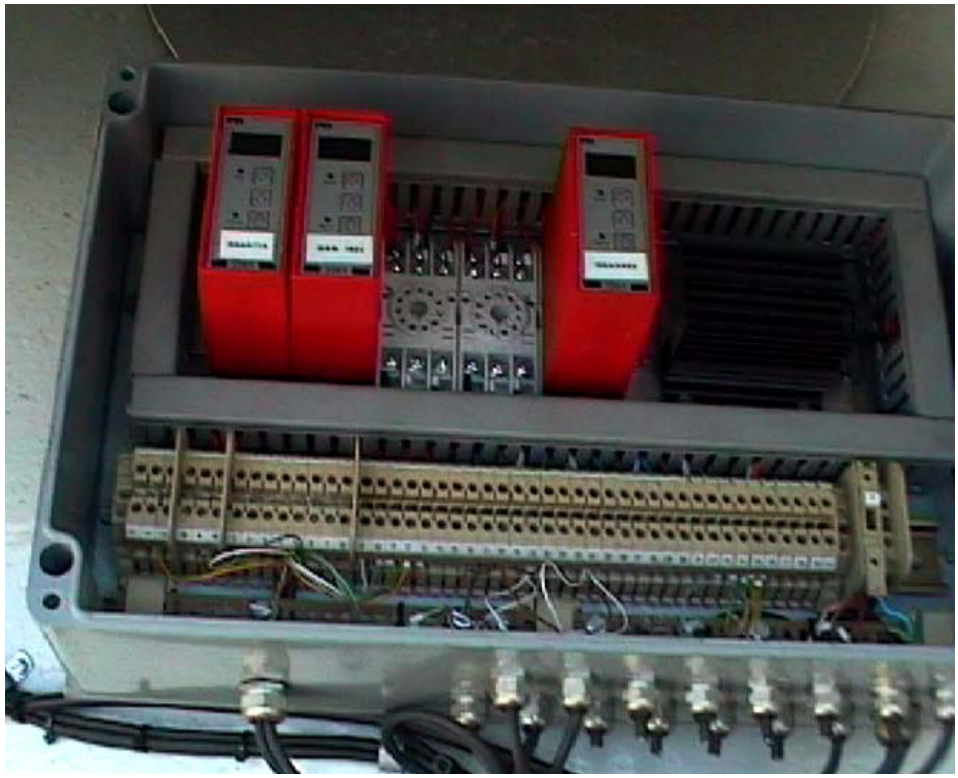

Figure 8. Blade root bending moment connector box.

Figure 9. Nacelle mounted box containing wireless network connection. Two antennas on the hub and two antennas in the nacelle were used to secure proper functionality. The two antennas in the nacelle can be seen to the right of the box. The antennas were (of course) mounted apart during operation of the measurement system.

2.2 Mounting the LEDs

Light emitting diods (LEDs) were attached to the surface of the blade to provide fixed reference points for the camera system.

Figure 10. Christer Enroth, FOI, is practising manoeuvring the sky lift.

Figure 11. The crane extends to 45 m height.

Figure 12. Electrical connection at the end of the fixed part of the blade appearing as two sheets of copper, The “stem” on the left is the tip pitching shaft.

Figure 13. Electrical connection on the extendable and pitching blade tip.

Figure 14. The copper tape is covered by insulating tape.

Figure 15. Blade-tip connection.

Figure 16. The LEDs were attached using epoxy adhesive.

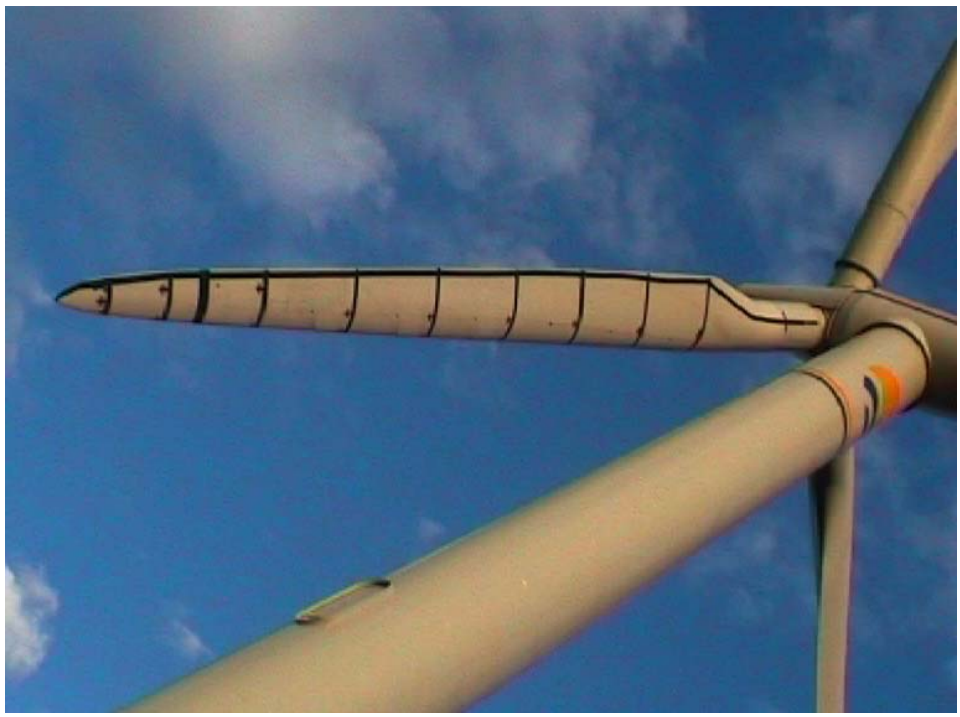

Figure 17. The instrumented blade.

Figure 18. LEDs in operation.

Figure 19. The instrumented blade at night captured by a video camera.

2.3 Equipment in tower base and cabin

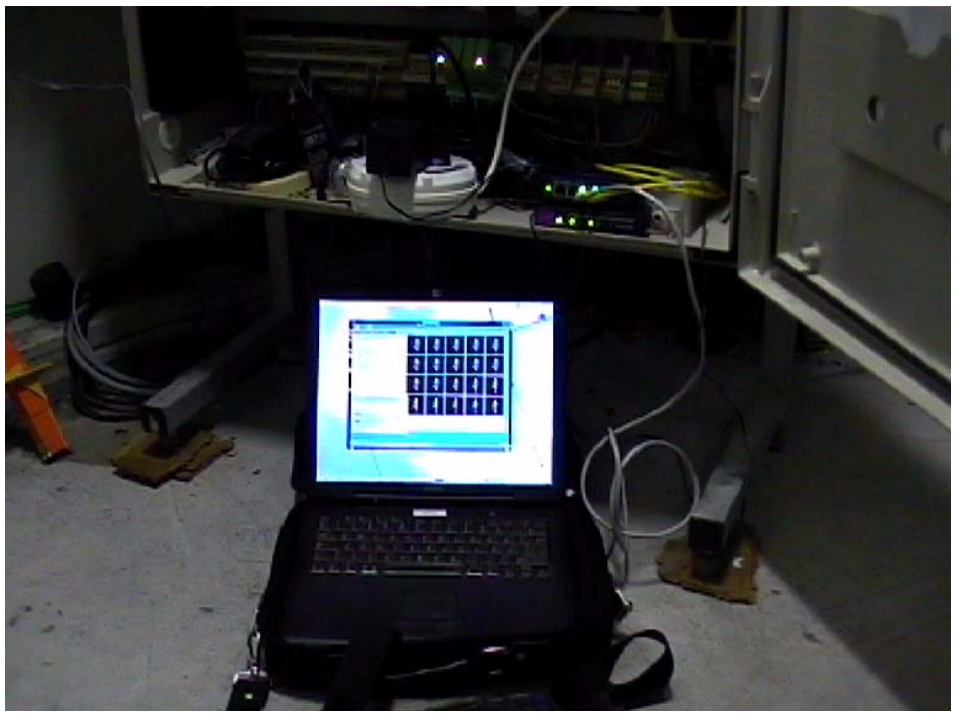

Figure 20. Network connection in tower base. A sequence of blade images are shown on screen.

Figure 21. Cabin with an external GPS-antenna for time synchronization with meteorological data.

Figure 22. Interior view of the cabin. The second computer is used by Uppsala university to store meteorological data.

2.4 Images from operation with LEDs

Images of the LEDs were taken every fifth minute between 2001-01-07 and 2001-02-10. The image analyses made it possible to produce an overlay which can be seen in Figure 23.

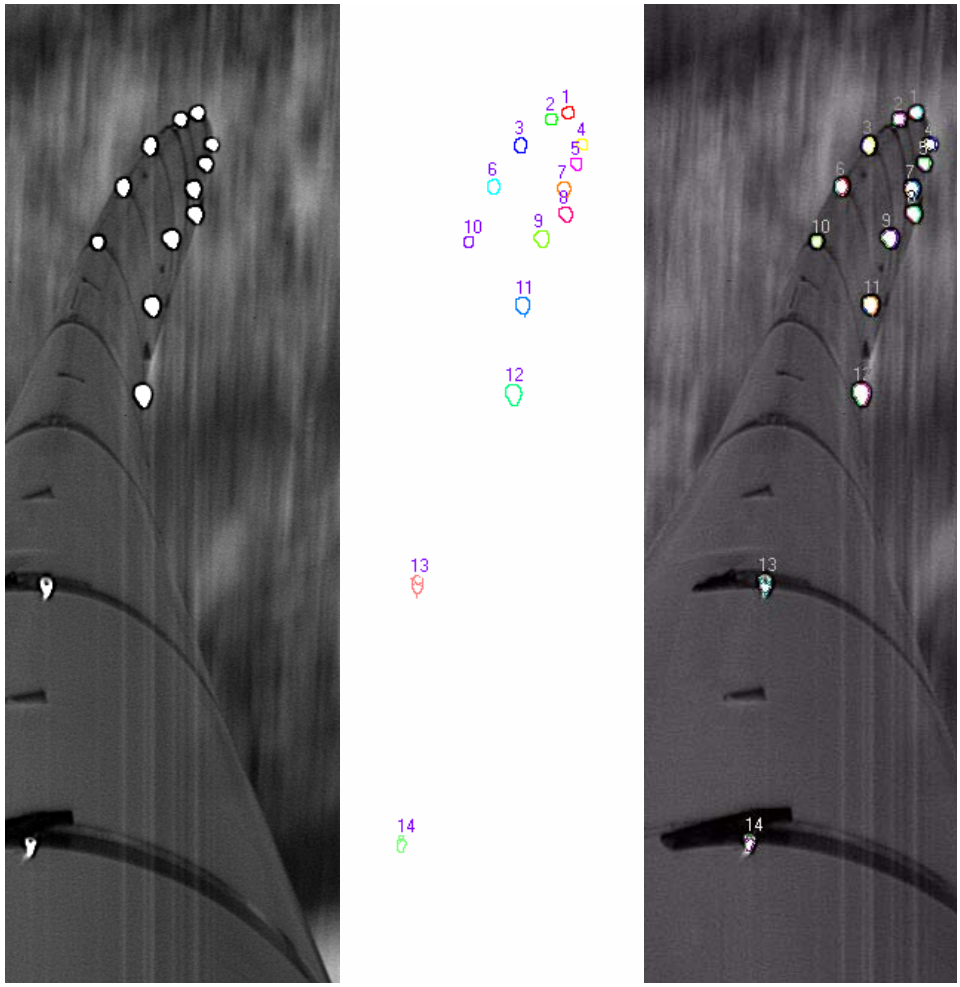

Figure 23. An example of analysed images of the LEDs.

An example of a sequence of images is shown in “VIBUD_LED_example.mov” on the CD. The sequence illustrates transition from daylight to darkness which, due to increased contrast and static light conditions, makes identification of individual LEDs easier.

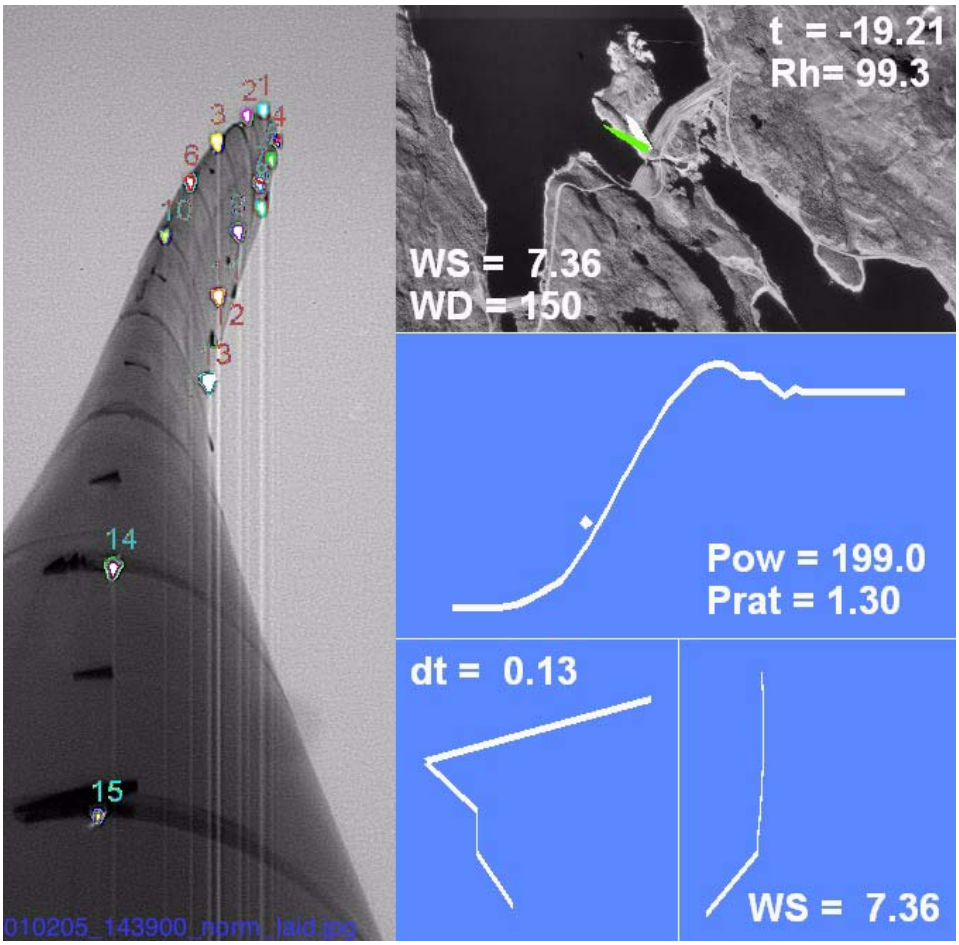

Figure 24. Image of LEDs mounted on the blade. All meteorological data is 10 minute averages except the green wind speed indicator which is sampled at 1 Hz.

2.5 Shifting gear box

After a month of operation of the LEDs the gear box had to be replaced. This also meant that the ordinary measurement system from the manufacturer could no longer be used as there were no slip rings for measurements mounted on the new gear box.

The tape covering the LED conductors at the blade tip had been worn down during operation. This finally resulted in a short circuit which turned off the LEDs.

Figure 25. The insulating tape came off partly close to the leading edge. The air speed at the tip is in the order of 300 km/h.

Figure 26. Corrosion broke the electrical connection at the blade tip.

The measurements were now stalled for almost two years due to a delay in ordering. This was not an ideal solution as data acquisition electronics are sensitive to corrosion.

2.6 Installing reflexes

The measurement system, which had been partly damaged by corrosion during 18 months at stand still, was repaired in December 2002. Prior to that, the blade was equipped with reflexes.

Figure 27. Green reflector tag close to a vortex generator 16 m from the blade tip.

Figure 28. Reflector tags at 2.1 m from the blade tip.

Figure 29. reflector tag attached 0.1 m from the blade tip.

A xyz model of the blade was available. The reflexes were “mounted” on this model using MatLab which made it convenient to compare the model with captured images.

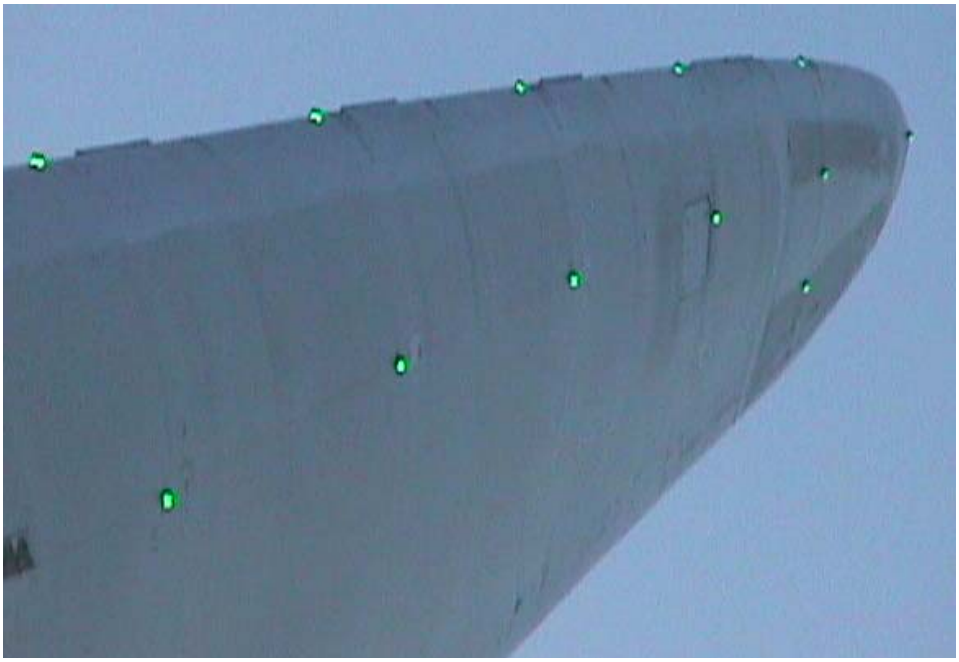

Figure 30. Reflector tags at 0.1, 2.1, 4,6, 8 &10 m from the tip. The outermost tags are also shown in Figure 28 and Figure 29.

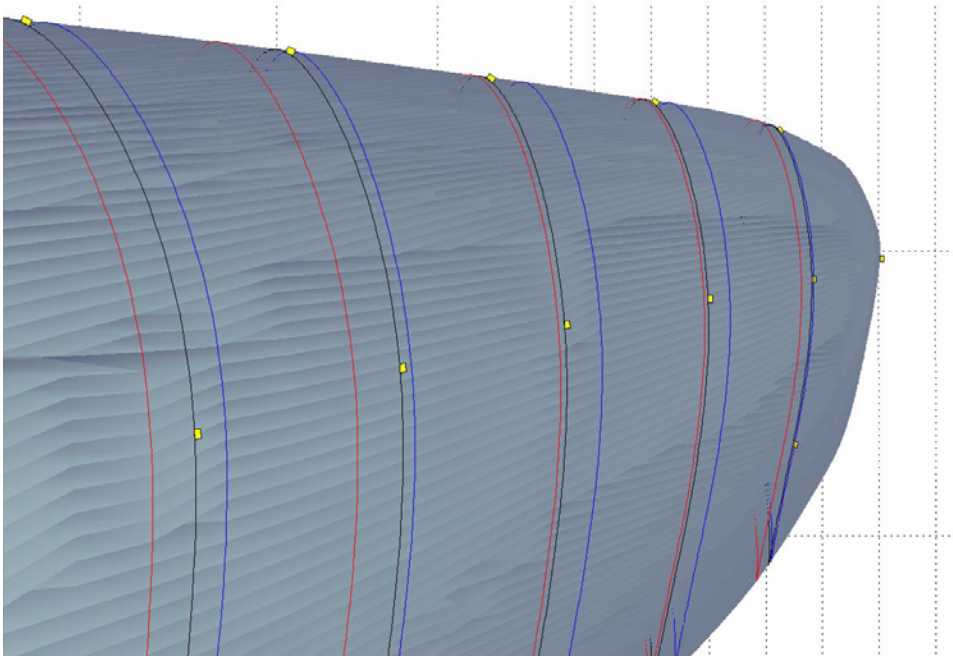

Figure 31. MatLab model of reflector tags at 0.1, 2.1, 4,6, 8 &10 m from the tip. The black lines indicate the interpolated airfoil at the radial of the reflector tags. The red and blue lines indicate the closest explicitly denoted airfoils. This is the same part of the blade as shown in Figure 30.

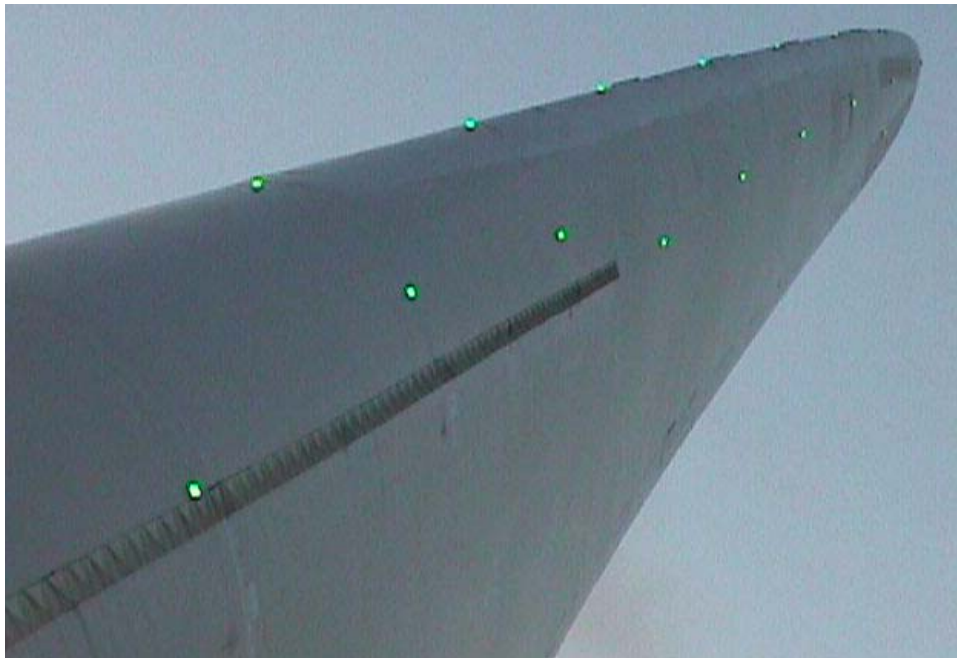

Figure 32. Reflector tags at 0.1, 2.1, 4,6, 8, 10, 12, 14 & 16 m from the tip. The innermost tag is also shown in Figure 27 on page 22.

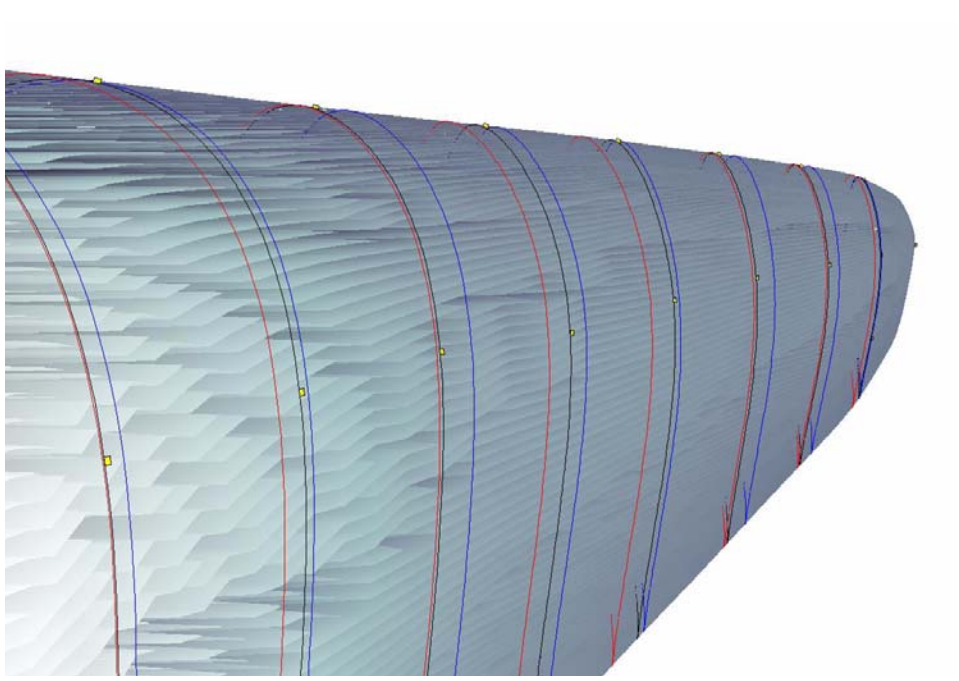

Figure 33. MatLab model of reflector tags at 0.1, 2.1, 4,6, 8, 10, 12, 14 & 16 m from the tip. The black lines indicate the interpolated airfoil at the radial of the reflector tags. The red and blue lines indicate the closest explicitly denoted airfoils. This is the same part of the blade as shown in Figure 32.

Several examples of captured video sequences are shown on the CD which accompanies this report.

3 Results

3.1 Long exposure time

As a first attempt, before the measurement system was programmed for fast image acquisition, a long exposure time was used to capture blade movements.

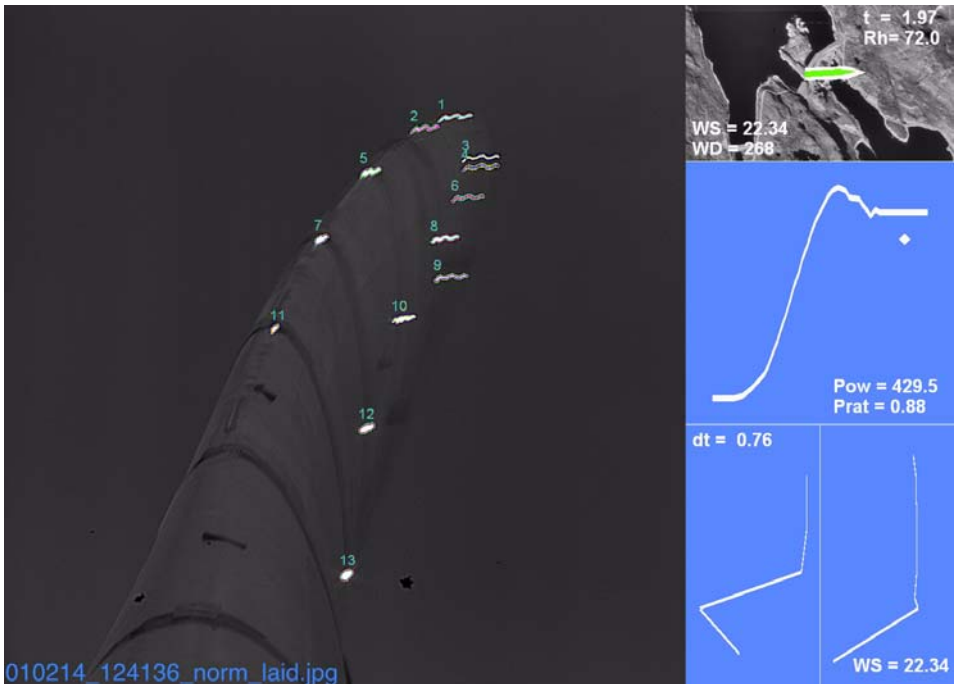

Figure 34. A 78 ms exposure time was used to capture blade movements.

A large flapwise deflection with an edgewise overlay is shown in Figure 34. The following image, Figure 35, shows the blade at the turning point in the flapwise direction.

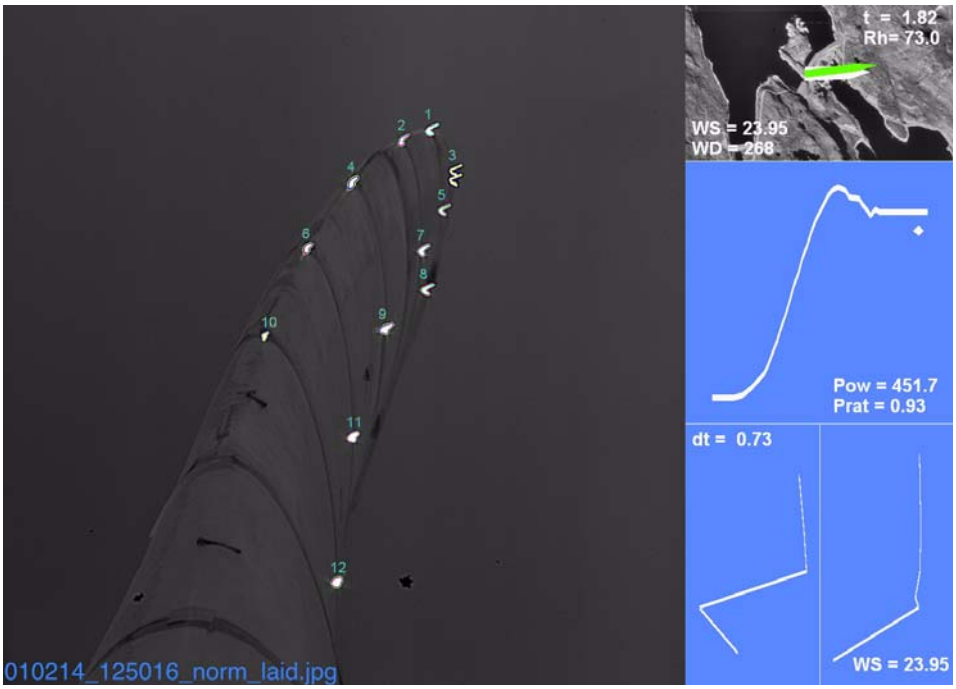

Figure 35. The blade at the turning point in the flapwise direction.

A long exposure time is useful for obtaining a basic overview of blade movements. It is, however, not possible to determine the instantaneous velocities as the image is integrated during a significant time period.

3.2 Sequences of images

50 images were captured during 4 seconds at the start of every hour. The image data are analyzed with respect to the number of objects found versus hour of day. As the number of actual targets was limited to LEDs and reflexes mounted on the blade it was possible to determine the reasonableness of the result.

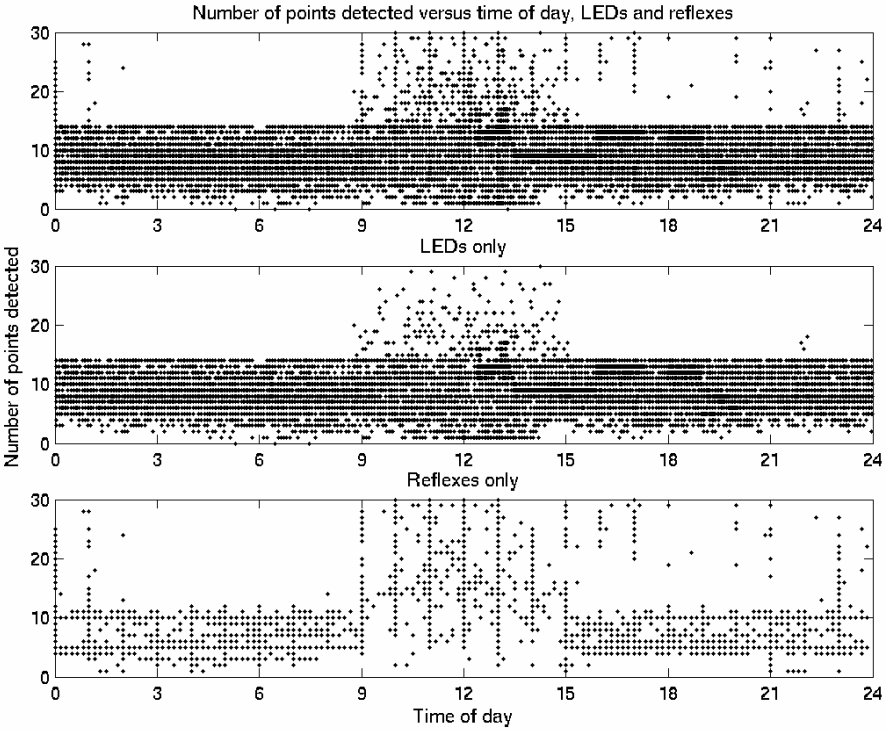

Figure 36. Number of objects found versus hour of day.

Figure 36 shows that daylight conditions made it more difficult to locate the targets. This result could have been improved by restricting the images to certain azimuthal angles thereby optimizing the aperture for a smaller variation of the incoming light. Storing nearby data points in bins and calculating statistical data is shown in Figure 37.

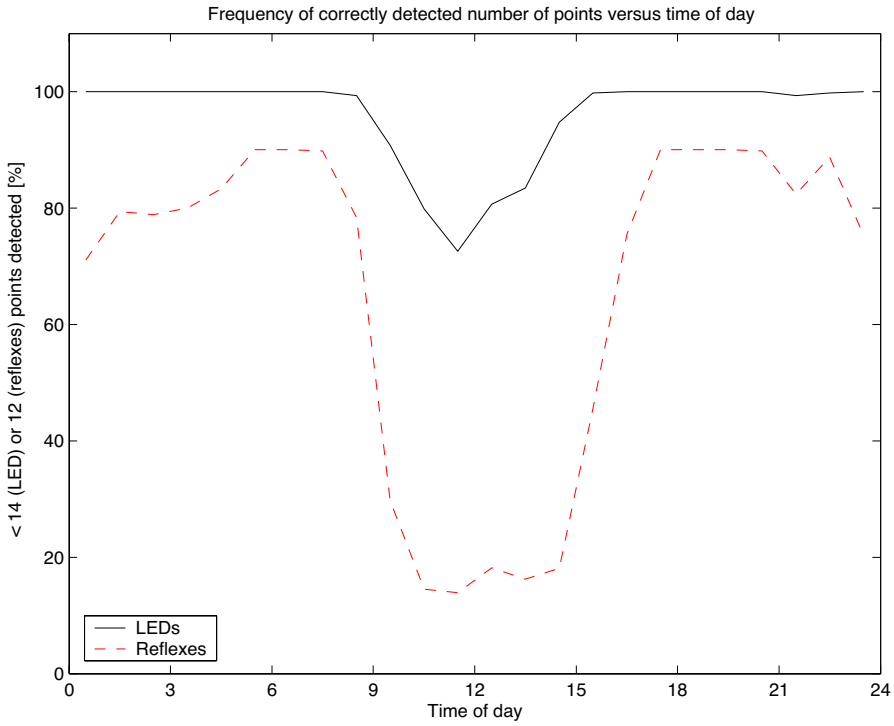

Figure 37. Frequency of correctly determined number of point versus time of day.

The LEDs were easier to locate due to a higher contrast in comparison with the reflexes. It was, on the other hand, more difficult to capture a distinct edge using the LEDs. This problem is either generic or can have been caused by overexposure of the LED images.

The number of points detected should increase as the blade deflects, Figure 38.

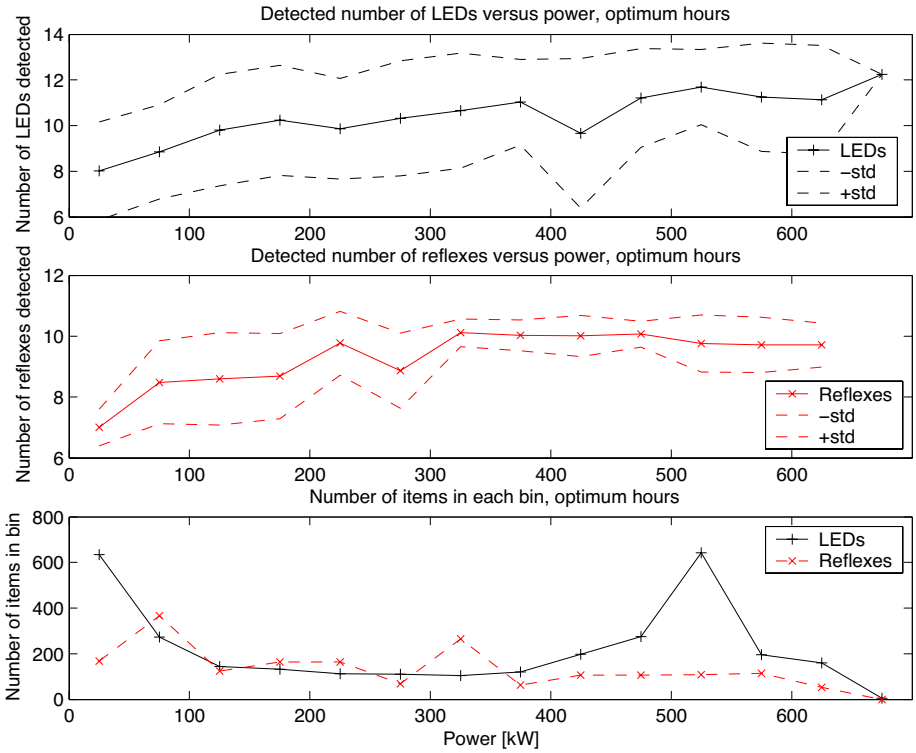

Figure 38. Number of points detected versus power.

The power produced below and above rated wind speed can be of equal magnitude at more than one wind speed. Figure 39 shows the number of points detected versus wind speed.

Figure 39. Number of points detected versus wind speed.

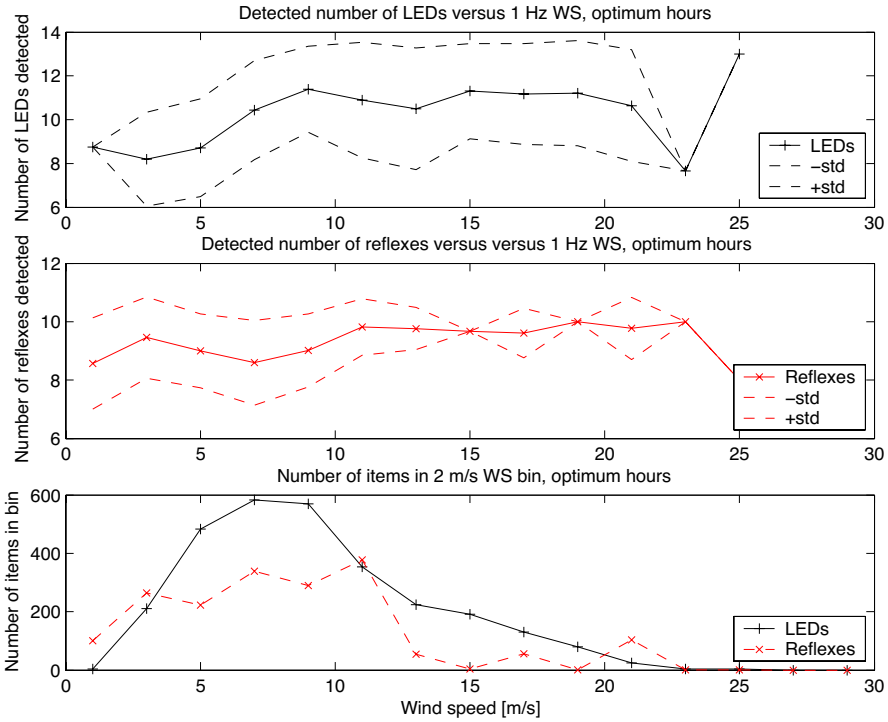

To ease tracking of points the analyzed data were sorted and selected with reference to low standard deviation among the points detected.

Figure 40. Case selected for analysis of blade movement is 4 sec sequence captured 2003-01-27 at 00.00.

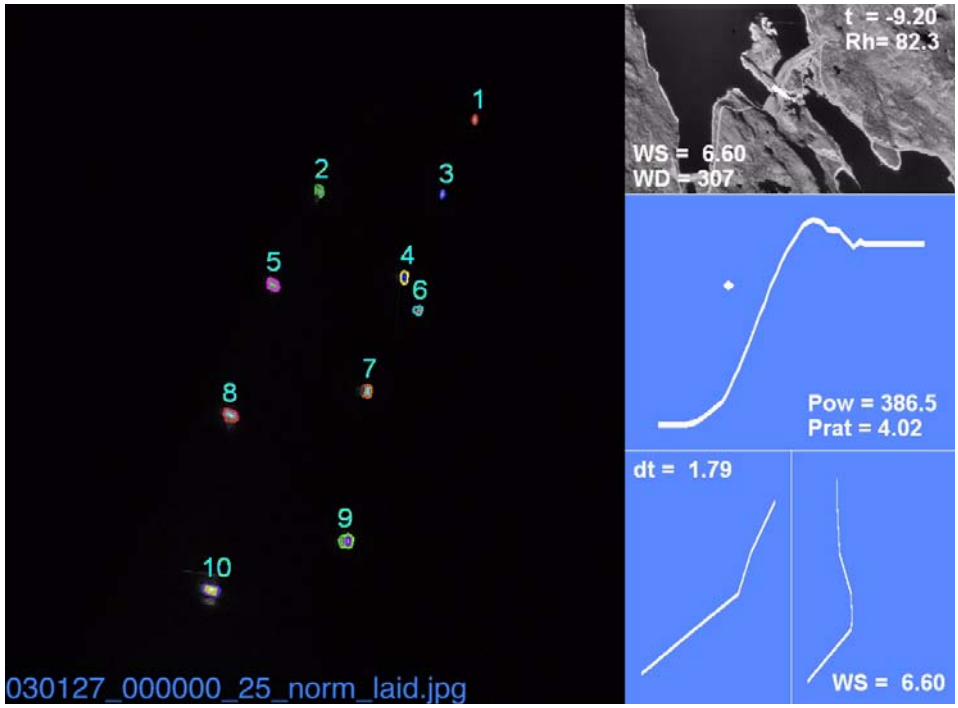

The co-ordinates of point #2 and #7 are shown in

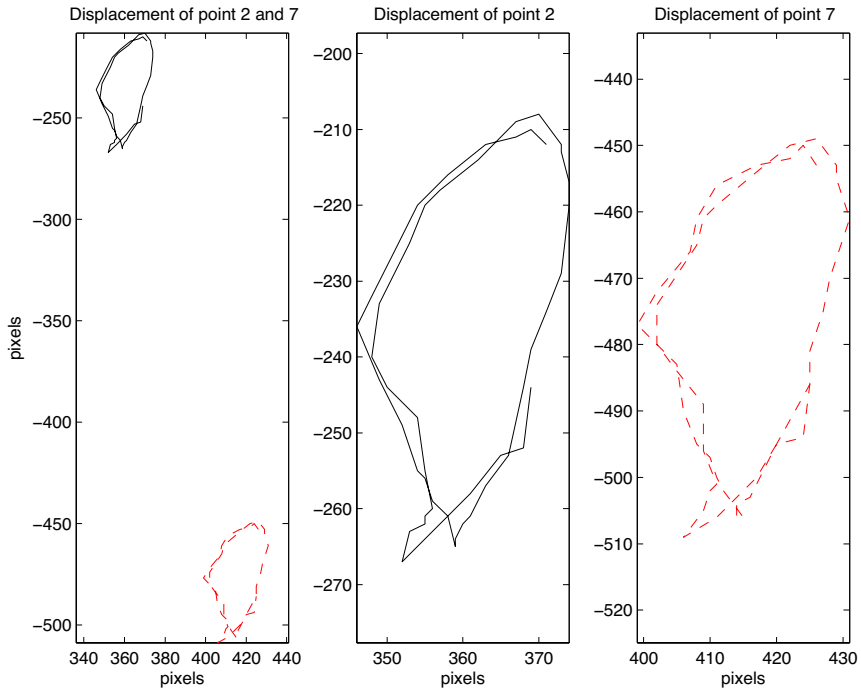

Figure 41. Displacement of point 2 and 7 in 50 sequential images, 4 sec sequence 2003-01-27 at 00.00.

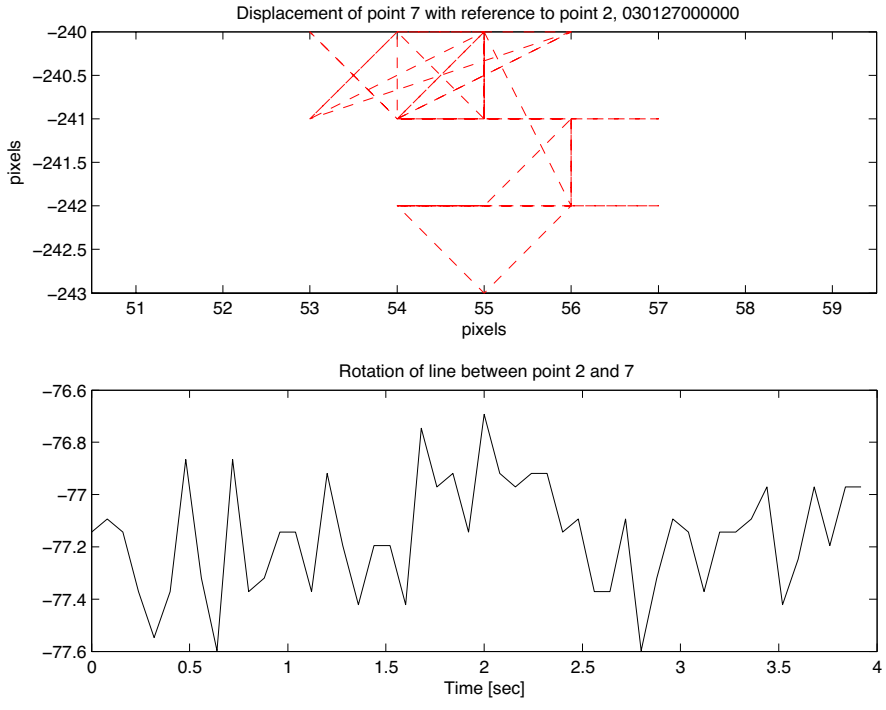

Figure 42. Displacement and angular variation of point 7 with reference to point 2 in 50 images, 4 sec sequence 2003-01-27 at 00.00.

The distance between the reflexes is known. This enables transformation to units of interest, such as mm, to be carried out.

The image analysis carried out and presented in this report shows that verification of simulation of blade movements is attainable. However, exact outdoor inflow conditions are extremely difficult to measure and it is therefore not possible to emulate every situation in detail. An increased knowledge of actual blade translation and rotation will nevertheless enable improvement of structural dynamics simulation codes. This is a need which will probably grow with the size of future turbines.

4 Icing

The intention was originally to evaluate loads and images jointly. Although this project proposal was accepted for financing, a significant delay in funding caused damage to the measurement system which initially had been installed during an earlier project. Hence, simultaneous loads and images have not been co-evaluated.

4.1 Examples of iced up blades

A few examples of an iced up wind turbine blade are presented along with an analysis of measured data. Figure 43 shows that ice accretion has occurred along the stagnation line. The increase in chord might be helpful in regaining performance lost because of the associated profile drag increase. It can be seen from the photo at stand still that open water is present nearby. Humidity from the lakes can cause severe icing to occur at Suorva before the surrounding waters have frozen over.

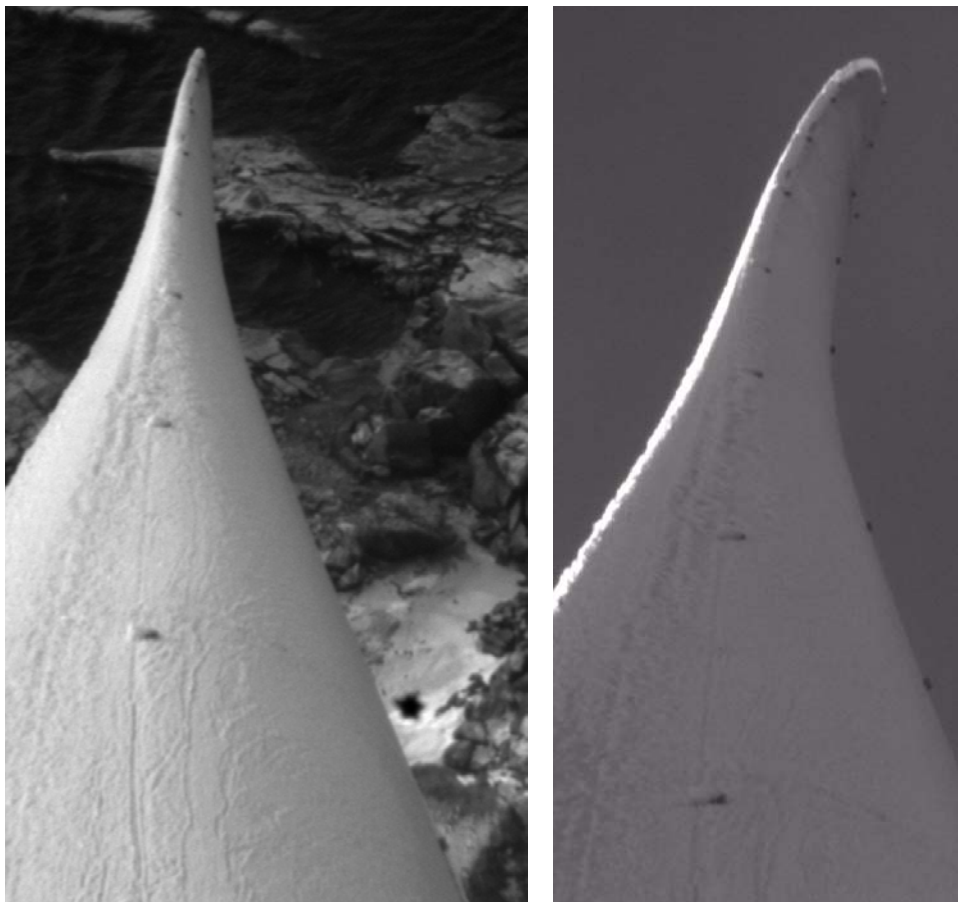

Figure 43. The iced up blade at stand still and during operation.

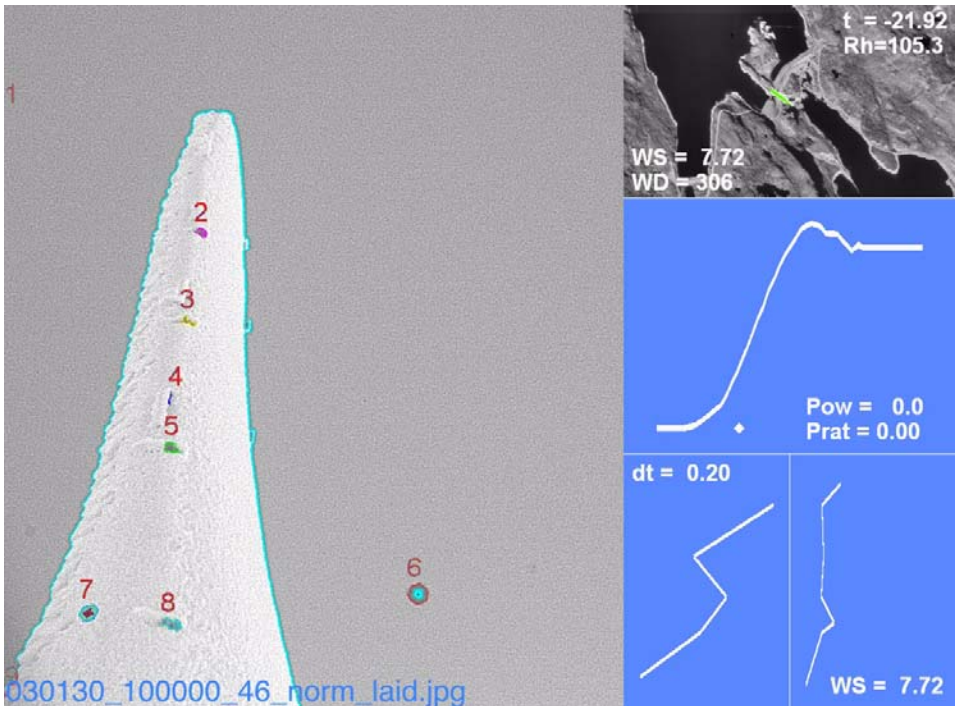

Figure 44. The iced up blade at stand still.

The turbine is heavily iced up and does not operate. In addition, one phase is missing in the anti-icing system which most probably causes less ice accretion on the other two blades thereby increasing the likelihood for vibrations to occur.

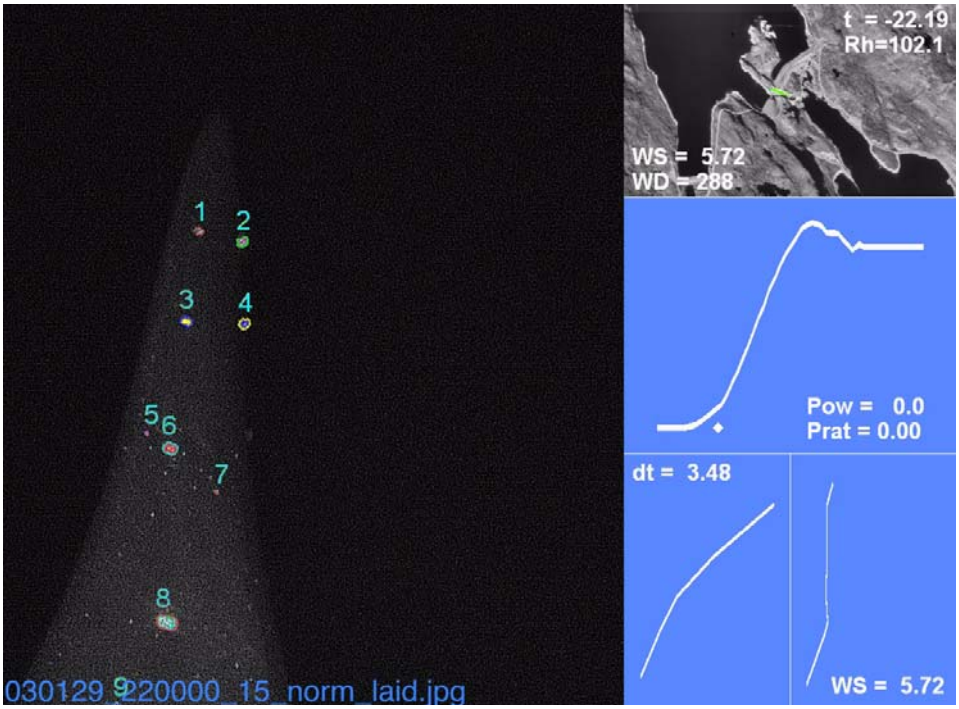

Figure 45. The iced up blade at stand still during night. The reflexes can be seen through the ice cover whereas they're less easy to detect during daylight. Icing occurred at a temperature around -20°.

4.2 Icing in measurements

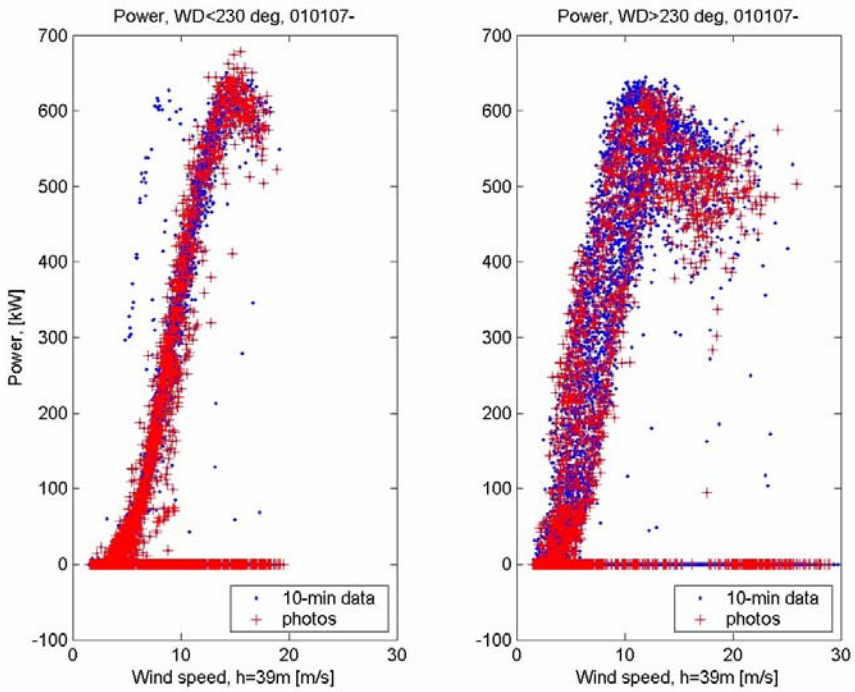

Figure 46. 10 minute averages of wind speed versus power. All situations are plotted in blue while conditions from which a photo is available are shown in red.

The difference between the two plots shown above is the wind direction. The measurement mast is sheltered in the second graph.

Wind speed measured using a heated anemometer can be compared to ditto measured by a non-heated anemometer to determine icing, Figure 47.

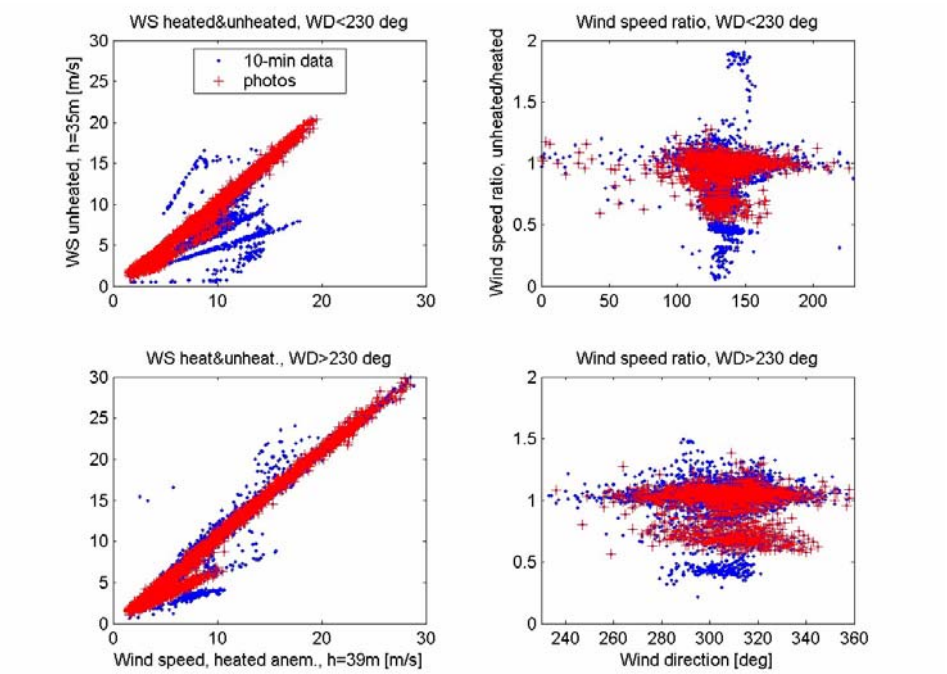

Figure 47. 10 minute averages of wind speed measured using a heated anemometer at h=39 m compared to non-heated at h=35 m. All situations are plotted in blue while conditions from which a photo is available is shown in red.

The lower wind speed measured at h=35 m in front of and behind the mast can also be caused by the tower shadow. Such sectors should be deleted in comparisons aiming at detecting ice.

There is an ice detector mounted on the nacelle, Figure 48. Data were divided into two opposite wind directions. One conclusion is that icing is indicated as low as close to -35°.

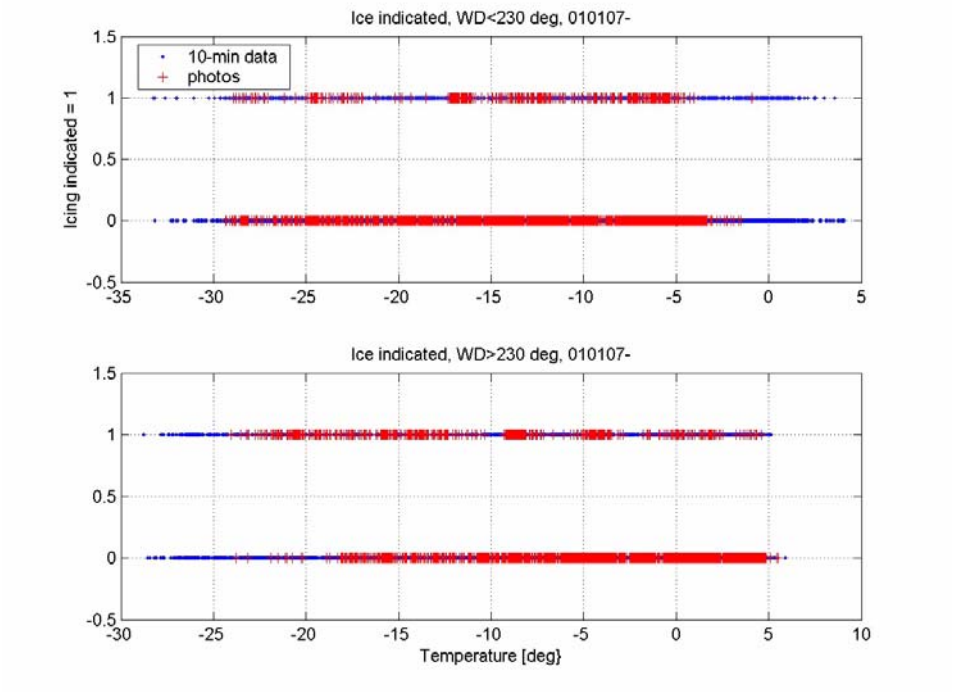

Figure 48. Icing occurs, according to the ice detector signal mounted on the nacelle at temperatures down to -35°.

A frequency analysis of the occurrence of icing versus temperature was not carried out.

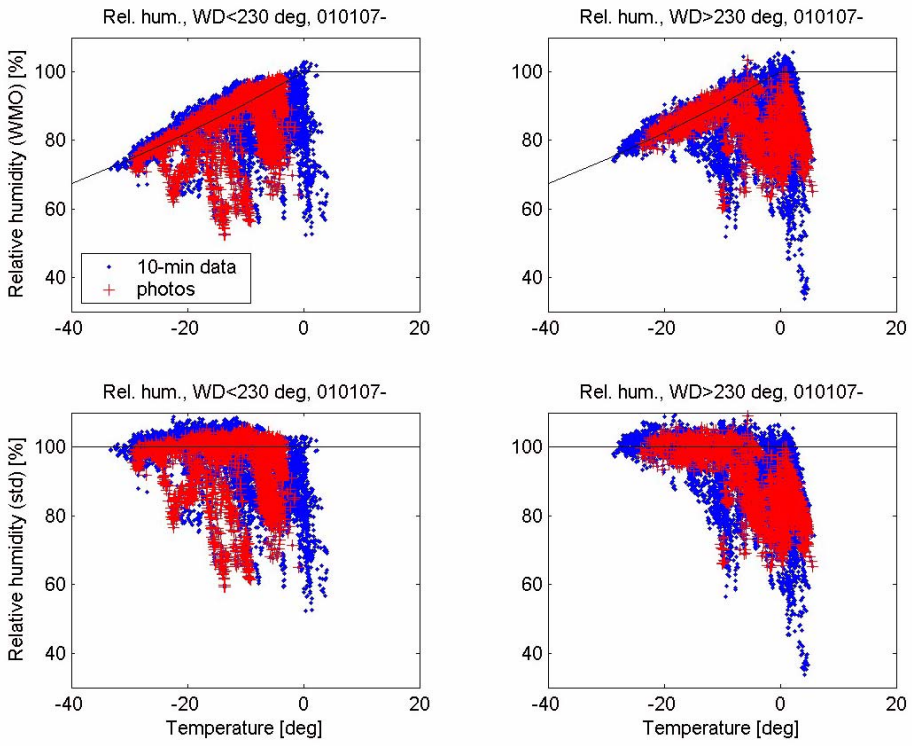

Figure 49. Relative humidity is traditionally measured not taking ice into account. Recalculating data below 0° with respect to ice might make it easier to determine when icing can be detected using ordinary meteorological instruments,

The relative humidity has since long been used to estimate the risk for icing. Recent findings by Makkonen et al. indicate that liquid water content and droplet size is of major importance for the formation of ice. However, these later parameters are, at present, not commonly measured at meteorological stations.

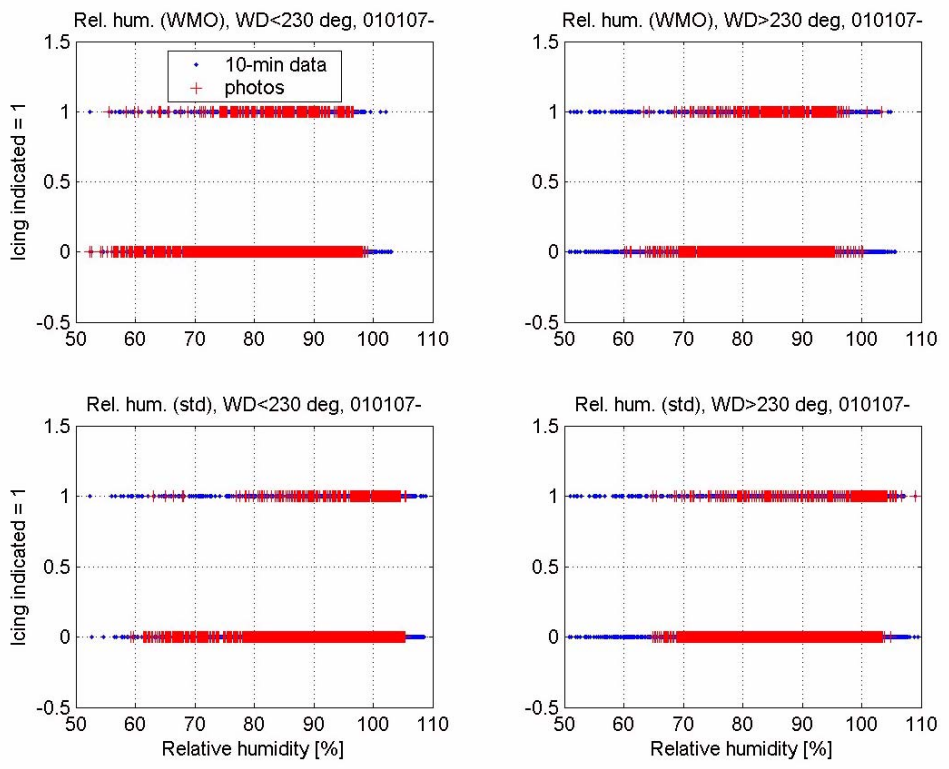

Figure 50. Icing detected by ice detector mounted on the nacelle versus relative humidity.

The ice detectors in use on wind turbines have not been sufficiently reliable and quick to detect icing. This is one reason why synoptic measurements, which means simultaneous measurements carried out over a large area, have not included measurement of icing. Verification of a new generation of ice detectors is to be carried out within the EU-programme COST 727 with the ultimate goal to include icing measurements in regular synoptic measurements.

References

[1] Ganander H., "Evaluation of Suorva Measurements 030121-030219", TG-R-04-03, Stockholm, 2004

[2] Dahlberg J-Å, Söderberg M., “Videofilmning av ett blad på WTS-3 i Maglarp”, FFA-A-788, Maglarp and Stockholm 1988-2002

[3] Furnée H et al, “Opto-Electronic Motion Measurement. A New Analysis Tool for Dynamic Field Testing of Wind Turbines”, DEWEC 2000

[4] “3-D Motion Analysis in Full Scale Wind Turbines - a new tool for dynamic in-field testing by non-contacting camera/computer measurement system”, EU-CRAFT/JOULE JOR3-CT97-7002, Aerpac Holding BV

[5] 3-D Motion Analysis in Full Scale Wind Turbines. A new tool for dynamic in-field testing by non-contacting camera/computer measurement system, JOR3961004, Aerpac Special Products BV